

57-63  
98  
188196

# Flexible Manipulator Control Experiments and Analysis

S. Yurkovich, Ü. Özgüner, A. Tzes, and P.T. Kotnik

Ohio State University  
Columbus, OH 43210

QM 59328

## Abstract

~~This presentation describes modeling and control design for flexible manipulators, both from an experimental and analytical viewpoint. From the application perspective, we report on an ongoing effort within the laboratory environment at The Ohio State University, where experimentation on a single link flexible arm is underway. Several unique features of this study are described here. First, the manipulator arm is slewed by a direct drive dc motor and has a rigid counterbalance appendage. Current experimentation is from two viewpoints: 1) rigid body slewing and vibration control via actuation with the hub motor, and 2) vibration suppression through the use of structure-mounted proof-mass actuation at the tip. Such an application to manipulator control is of interest particularly in design of space-based telerobotic control systems, but has received little attention to date. From an analytical viewpoint, we discuss parameter estimation techniques within the closed-loop for self-tuning adaptive control approaches. Also introduced is a control approach based on output feedback and frequency weighting to counteract effects of spillover in reduced-order model design. A model of the flexible manipulator based on experimental measurements is evaluated for such estimation and control approaches.~~

ms described,

is described.

ms described.

## 1. Introduction

Traditionally, robotic manipulator arms have been modeled as being composed of rigid links, with co-located actuators and sensors, towards the goal of ensuring stable and reliable control. In order for typical manipulator arms to maintain this rigid property as modeled while carrying payloads, the mechanical design requires large and massive links. This in turn dictates that the torques applied by the joint actuators be large, and heavy, usually geared motors are needed for actuation. Moreover, the controller for such a system is forced to move the arm slowly and deliberately so as to prevent any swaying or vibrations.

In recent years there has been much interest in using light-weight, higher performance arms for both commercial and space-based applications, leading to the study of flexible manipulator control. The advantages of flexible robotic manipulators are many, including faster system response and lower energy consumption, smaller actuators and overall trimmer mechanical design, reduced nonlinearity effects due to elimination of gearing, less overall mass and generally less cost. Obvious tradeoffs, however, complicate the issue of flexible manipulator control, primarily centering on the design of controllers to compensate for, or to be robust in the presence of flexure effects. With the advent of advanced computational resources, strides are currently being made towards solution of the many problems associated with control design.

Control design for lightweight flexible manipulator arms has gained the attention of control theorists only recently, and several approaches have emerged. Most prominent are approaches which either linearize and truncate for controller design, or solve the nonlinear robotics problem for rigid link motion control and treat the flexible dynamics separately. For example, the problem of observation spillover and truncation error effects is treated in [1], where in simulation studies a linear feedback scheme around a reduced order model is introduced for a single-link manipulator. In [2] control of the rigid motion is accomplished via state feedback linearization whereas vibrational dynamics are treated as disturbance effects. Several other analyses have appeared along these basic lines, using various approaches [3,4,5,6,7]. From an applications viewpoint, however, only a few studies have been documented for parameter estimation, system identification, and control. Most prominent among these are the works of Book, et al. [8,9,10,11] for time optimal slew experiments, related studies at JPL in flexible beam control [12,13], Schmitz and Canon [14] using non-co-located and tip position sensing in the control algorithm, and several studies conducted at NASA LaRC [15,16].

In this presentation we report on progress made to date on modeling and control design for flexible manipulators, both from an experimental and analytical viewpoint. Specifically, we discuss the ongoing effort within the Control Research Laboratory at The Ohio State University, where experimentation on a single link flexible arm is underway. The manipulator arm is slewed by a direct drive dc motor and has a rigid counterbalance appendage. Current experimentation is from two viewpoints: 1) rigid body slewing and vibration control via actuation with the hub motor, and 2) vibration suppression through the use of structure-mounted proof-mass actuation at the tip. Real-time parameter estimation techniques, within the closed-loop for self-tuning adaptive control, is under investigation and is described briefly here. In these initial studies, a model of the flexible manipulator based on experimental measurements is evaluated.

## 2. Experimental Setup

### 2.1 Apparatus

Within the Control Research Laboratory at The Ohio State University, several experimental configurations are under study for system identification and slewing and vibration control for flexible mechanical structures. In this presentation we focus on experimentation and simulation analysis with a single link flexible arm, depicted in Figure 1. The arm is made of 0.0625 inch

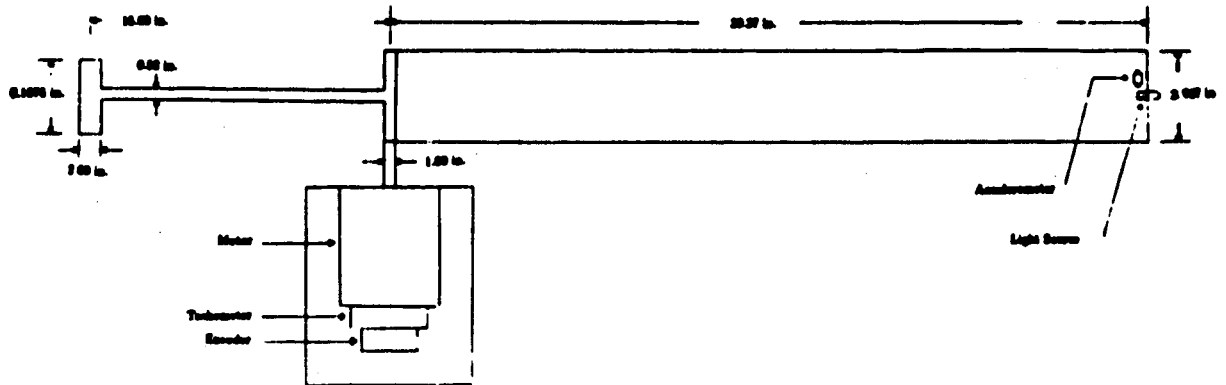


Figure 1: OSU Flexible Arm

thick aluminum and is counterbalanced with a rigid aluminum appendage with mass equal to that of the arm. Hub actuation is accomplished by a 3.4 ft-lb *direct drive* dc motor which has an optical encoder with a quadrature digital output to sense motor shaft position, and a tachometer to measure motor shaft speed. This, then, allows both hub position and velocity feedback for control. Strain gauges (for monitoring and parameter estimation) and an accelerometer are placed along the arm, and a 512-element CID linear array camera with RS-422 interface is used for sensing the tip position by observing the lamp fixed to the tip of arm. With such a scheme, the tip sensing mechanism (camera) is utilized in verification and tuning of the predicted endpoint position. A related objective for this setup is to achieve control without camera information feedback, with for example rate and acceleration sensing feedback, for application in space-based manipulator systems where off-structure reference for sensing is impractical.

Some characteristics of the arm are given below.

Table 1: Arm Characteristics

|  |  |
|--|--|
| Material                               | 6061-T6 Aluminum                       |
| Modulus of Elasticity                  | $68.944 \times 10^9$ N/m <sup>2</sup>  |
| Cross Sectional Area Moment of Inertia |  |
| Flexible Arm                           | $3.350 \times 10^{-11}$ m <sup>4</sup> |
| Rigid Appendage                        | $2.427 \times 10^{-6}$ m <sup>4</sup>  |
| Lengths                                |  |
| Flexible Arm                           | 1.0 m                                  |
| Rigid Appendage                        | 0.381 m                                |

The unique features of the structure are the direct drive mechanism, chosen to minimize effects of backlash and other nonlinearities due to gearing, and the counterbalance appendage, which provides a more realistic model of application-oriented structures. Such a hybrid structure does, on the other hand, pose unique problems for analytical modeling.

Two computing environments are available in the laboratory for real-time control and data acquisition. The first such system is an IBM AT which uses different combinations of several custom-built cards in addition to the A/D equipment. These cards include a controller for the slewing motor with electronics utilized in processing data received from the linear-array camera. Another card, designed in-house, processes strain gauge and accelerometer data, and includes a low-noise, high-gain amplifier with a low pass

filter and excitation to the bridge circuitry. A third custom board is used to drive the proof-mass actuators (discussed in [17] and later in this presentation). The board receives an analog voltage from the D/A and amplifies it to a current which is adequate to drive the actuators. The linear array camera is interfaced to the computer using a custom board which converts the camera's serial data stream to a number corresponding to the position of the beam endpoint. The second computing system is the MicroVax II, equipped with commercially available A/D-D/A boards and real-time operating system software. For the study presented here, the data acquisition is carried out using the IBM AT due to the availability of the camera interface electronics.

### 2.2 Modeling and Frequency Response

For purposes of finite element modeling studies, the arm is analyzed in two separate components, those being the flexible arm itself and the rigid counter balance. The cylindrical mass at the end of the rigid component is modeled as a point mass, and the two components are connected at the pinned joint (motor shaft). For the FEM analysis, each component is modeled as a two-dimensional elastic beam, and the software package ANSYS [18] was used to generate the first five modes of the system shown in Table 2 below. We note that torsional modes were assumed to be insignificant, and were therefore neglected in the analysis. The principle advantage to modeling the arm in this manner is that the effects of the counter balance in the static characteristics are included. Several other approaches were utilized, such as considering the joint at the motor shaft to be a fixed point (clamped free), negating any effect the counter balance may have on the beam dynamics. Experimental results (described below) indicate that the former approach, described above, gives the closest match to measured responses.

For purposes of comparison, several experiments were conducted in testing response characteristics of the apparatus. An open loop frequency response was found by applying a sinusoidal system input torque (varying the motor current), and recording measurements of the tip position; the procedure is similar to that employed in [14]. Data was taken over the range 0.2 Hz to 13.0 Hz, in steps of 0.1 Hz, and the results are shown in Table 3. The system poles and zeros were found by noting the frequencies which produced maximum and minimum tip deflection, respectively. An inherent assumption in this technique is that the damping of the beam is very small (this fact was experimentally verified in an independent study [19]). The damping ratio calculations represented in the table are based on the assumption that excitation near a modal frequency will result in the response showing primarily only that particular modal frequency.

Table 2: FEM Results

| Mode | Frequency (Hertz) |
|------|-------------------|
| 1    | 2.0091            |
| 2    | 8.2509            |
| 3    | 23.1187           |
| 4    | 46.5677           |
| 5    | 79.5244           |

Table 3: Frequency Response Data

| Minimum Tip Response | Maximum Tip Response | Damping Ratio |
|----------------------|----------------------|---------------|
| 3.0 Hz               | 1.2 Hz               | 0.139         |
| 10.3 Hz              | 7.6 Hz               | 0.050         |
| 11.3 Hz              | 12.0 Hz              | 0.008         |

The open loop step response (in position) of the arm was found by rotating the motor shaft through an angle of 10 degrees and measuring the tip deflection from its nominal value (initial point). After this maneuver the motor holds the new position (that is, is servoing) since the local feedback loop is active. Figure 2 illustrates a plot of the step response. Note that while the torque is applied at the hub at time  $t = 0$ , the tip deflection response is delayed by approximately 30 milliseconds and, in fact, initially moves in the direction opposite that of the hub rotation. The step responses indicates a settling time of about one minute. A fast Fourier transform of the data allows linear identification of the first two modal frequencies; these occur at 1.18 Hz and 7.5 Hz, respectively. Figure 3 shows the result of the FFT for the tip position in the step response test. We note that the rigid body mode (dc component) due to the pinned joint has been subtracted out of the FFT plot for clarity.

## 3. Control Analysis

### 3.1 Problem Formulation

Consider again the single link flexible manipulator system described above, redrawn in Figure 4. The displacement of any point along the arm is given by the hub angle  $\theta(t)$  and the deflection  $\phi(x, t)$  measured from the line  $\partial \bar{x}$ . We assume that only transverse vibration is present and that the deflection due to this vibration is small. Let  $L$  be the arm length so that in general terms

$$y(x, t) = \phi(x, t) + x\theta(t) \quad (1)$$

$$\frac{\partial^2}{\partial x^2} \left[ EI(x) \frac{\partial^2 \phi(x, t)}{\partial x^2} \right] = -m_x A \frac{\partial^2 \phi(x, t)}{\partial t^2} \quad (2)$$

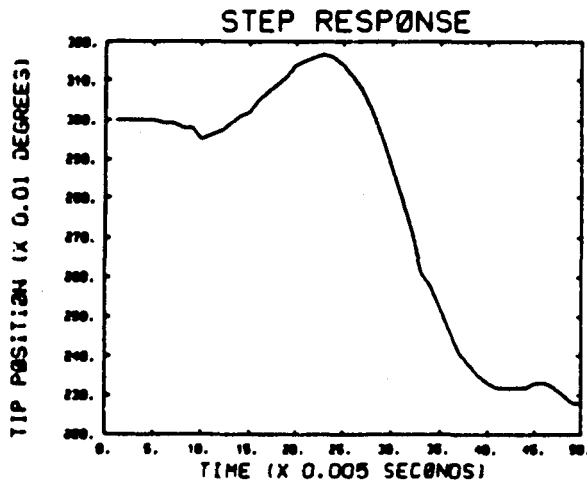


Figure 2

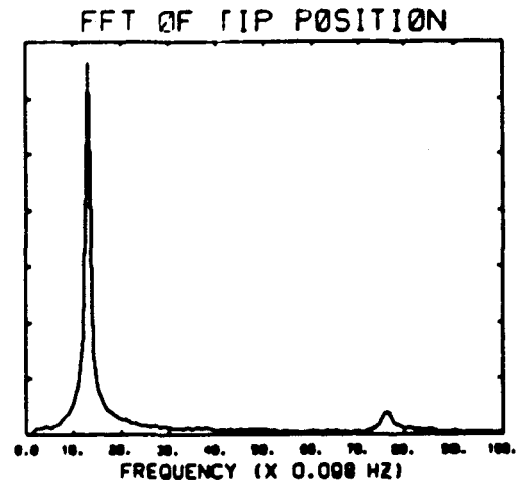


Figure 3

where  $EI(x)$  is the elastic stiffness,  $A$  is the cross-sectional area, and  $m_l$  is the mass density. For the mechanical configuration under consideration, (2) must satisfy the boundary conditions

$$\phi(0, t) = 0 \quad ; \quad EI(x) \frac{\partial^2 \phi}{\partial x^2} \Big|_{x=0} + T - I_H \ddot{\theta} = 0 \quad ; \quad EI(x) \frac{\partial^2 \phi}{\partial x^2} \Big|_{x=L} = 0 \quad ; \quad EI(x) \frac{\partial^3 \phi}{\partial x^3} \Big|_{x=L} = 0 \quad , \quad (3)$$

where  $T$  is the torque at the hub and  $I_H$  is the actuator inertia. Accordingly, (2) may be put into the familiar form for the generalized modal coordinates  $q(t)$  as

$$M \ddot{q} + D \dot{q} + K q = B f \quad , \quad \dot{q} = [\dot{q}_1, \dot{q}_2, \dots, \dot{q}_n]^T \quad , \quad (4)$$

where  $M$  is the mass matrix,  $K$  is the stiffness matrix, and  $D$  contains terms associated with the damping. For position and velocity measurements (in the  $y$  direction) the solution to (4) is approximated by

$$y(x, t) = \sum_{k=0}^n J_k(t) v_k(x) \quad (5)$$

for the eigenfunctions  $v_k(x)$ , including the rigid body mode at  $k = 0$ , and the  $J_k(t)$  are chosen to minimize the mean-square error upon substitution into (1).

Under the unitary transformation  $\Phi$ , then, we use the notation  $q$  now to represent the state in the state variable formulation of (4) as

$$\begin{bmatrix} \dot{q} \\ q \end{bmatrix} = \begin{bmatrix} 0 & I \\ -\Omega^2 & -\Phi^T D \Phi \end{bmatrix} \begin{bmatrix} q \\ \dot{q} \end{bmatrix} + \begin{bmatrix} 0 \\ \Phi^T B \end{bmatrix} f \quad , \quad y(t) = C \begin{bmatrix} q \\ \dot{q} \end{bmatrix} \quad , \quad (6)$$

where  $\Omega^2 = \Phi^T K \Phi$  is an  $n \times n$  diagonal matrix containing the squares of the modal frequencies  $\omega_1, \omega_2, \dots, \omega_n$  along the diagonal, and  $y(t)$  is the measurement vector. Upon rearrangement, we may write (6) in the manner

$$\begin{bmatrix} \dot{q}_0 \\ \dot{q}_1 \\ \dot{q}_2 \\ \vdots \\ \dot{q}_n \\ \dot{q}_n \end{bmatrix} = \begin{bmatrix} 0 & 1 & & & & \\ 0 & 0 & & & & \\ & & 0 & & 1 & \\ & & \omega_1^2 & & -2\zeta_1 \omega_1 & \\ & & & & & \ddots \\ & & & & & & 0 & & 1 \\ & & & & & & -\omega_n^2 & & -2\zeta_n \omega_n \end{bmatrix} \begin{bmatrix} q_0 \\ q_1 \\ q_2 \\ \vdots \\ q_n \\ q_n \end{bmatrix} + \begin{bmatrix} 0 \\ 1 \\ 0 \\ b_1 \\ \vdots \\ 0 \\ b_n \end{bmatrix} f \quad , \quad (7)$$

We note that in (7) the rigid body mode has been included. Since the only control input for this example is the torque, then  $f = T$ . Finally, the matrices  $C$  and  $\Phi^T B$  are given by

$$C = \begin{bmatrix} L & 0 & v_1(L) & 0 & \dots & v_n(L) & 0 \\ 0 & 1 & 0 & \frac{v_1'(0)}{L} & \dots & 0 & \frac{v_n'(0)}{L} \end{bmatrix} \quad , \quad \Phi^T B = \begin{bmatrix} 1 & \frac{v_1'(0)}{L} & \dots & \frac{v_n'(0)}{L} \end{bmatrix}^T \quad (8)$$

### 3.2 Parameter Estimation

The fundamental issue in the mathematical formulation of flexible mechanical structures lies in the fact that such distributed parameter systems must be identified (controlled) with only a limited number of sensors (actuators). Indeed, for the analysis of the single-link flexible arm we typically consider hub actuation only, and tip position and/or hub velocity measurements to be employed in modeling and feedback control. Moreover, without reliable models for the control design the analysis becomes even more difficult. Philosophically, there are several different views to take in the control design. One approach is to construct a controller that is reasonably robust in the presence of modeling uncertainties and spillover, and yet simple enough in structure to be easily implementable (for example the variable structure control approach [20]). Another approach is to perform system identification exercises to model the system as accurately as possible prior to control design. A third approach is a combination of the first two: estimate the system parameters on-line (in the closed loop) and base the control design on the resulting model. This last viewpoint is often referred to as Self-Tuning Adaptive Control (STAC).

In the STAC approach, the manipulator dynamics are represented by linear discrete-time models, affording the primary advantage that the controller design is inherently digital in nature. In the application to flexible structures, tuning parameters include combinations of the damping and modal frequencies, or some combination of other free parameters which make up the manipulator model. Our approach to the parameter estimation problem involves recursive least squares methods with covariance resetting. That is, in order to maintain a fast overall convergence rate, the covariance of the estimates is reset at regular intervals in the algorithm. Such a scheme is particularly attractive for the manipulator control problem due to the time-varying nature of the tuning parameters during slew maneuvers and varying payload exercises. Experimental studies of the parameter estimation and STAC approach for the arm described above are presently underway. In the following we present simulation results which indicate avenues to pursue regarding implementation.

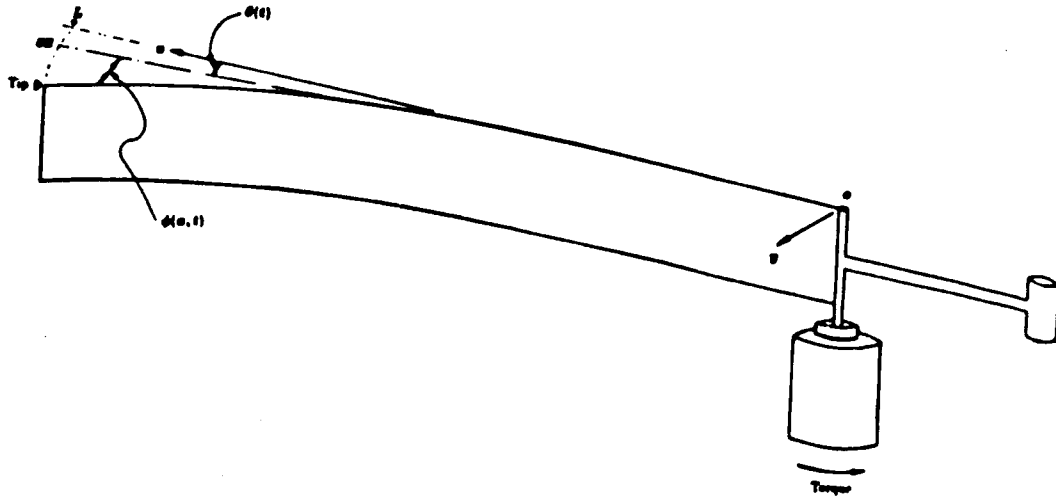


Figure 4: Deflection  $\phi(x, t)$ , Slew angle  $\theta(t)$

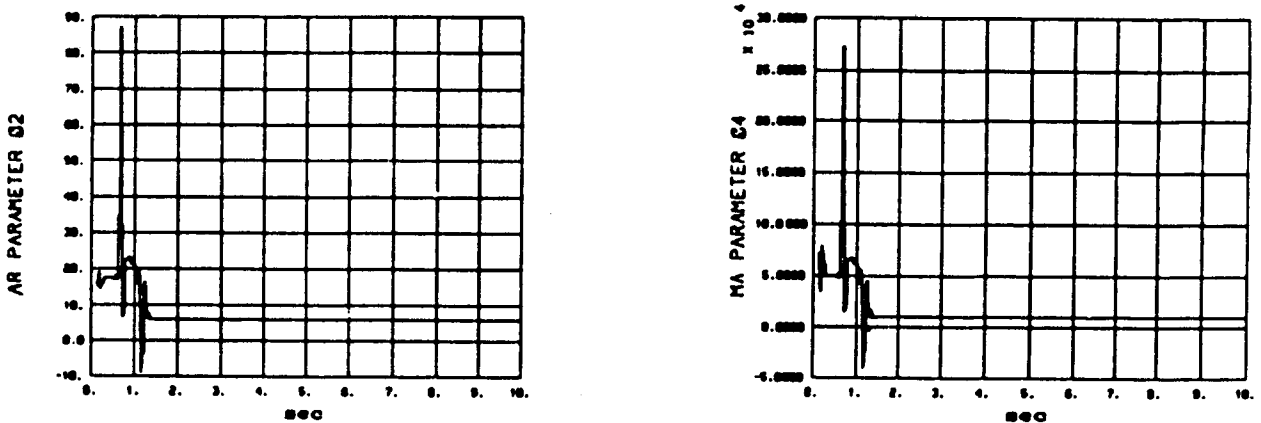


Figure 5: Parameter Estimation Simulation Results



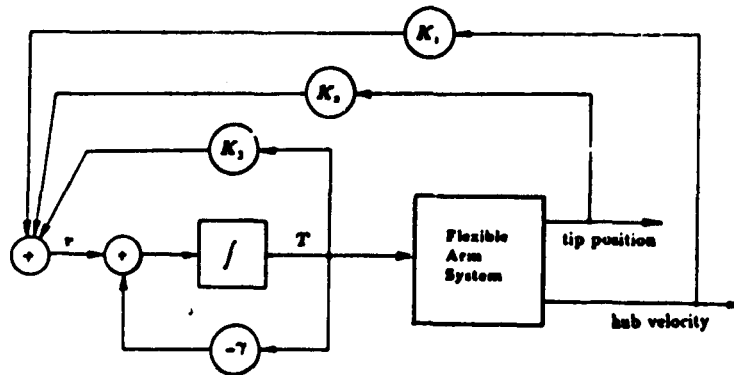


Figure 6: Output Feedback Scheme

$$\dot{v}(t) = \begin{bmatrix} L & 0 & \psi_1(L) & 0 & \dots & \psi_n(L) & 0 & 0 \\ 0 & 1 & 0 & \frac{d\psi_1(0)}{dx} & \dots & 0 & \frac{d\psi_n(0)}{dx} & 0 \\ 0 & 0 & 0 & 0 & \dots & 0 & 0 & 1 \end{bmatrix} \begin{bmatrix} q \\ \dot{q} \\ T \end{bmatrix}, \quad (12)$$

where the new measurement  $\dot{v}(t)$  now includes the torque  $T$ . Incorporating the system of (11)–(12) into the output feedback structure of Figure 6 (and subsequent solution of the corresponding Lyapunov equation) allows the off-line calculation of the feedback gains from minimization of (10) by an appropriate nonlinear optimization routine.

We consider now a simulation of the flexible arm system, using a five-mode model from the FEM as the "truth model", from which measurements are taken and fed back in the output feedback scheme. The controller design for this example is based on the reduced system of rigid mode plus first flexible mode, and the resulting control is then tested against the full-order truth model to illustrate the effects of the frequency weighting approach in reducing spillover. A conjugate gradient method is used in the optimization portion of the design, and the final values obtained for the control law (with  $\gamma = 4$ ) are  $K_1 = -110.09$ ,  $K_2 = -111.53$ ,  $K_3 = -88.83$  (feasible values for the system under consideration) for the cost which reached a minimum after approximately 3000 iterations. The results using this controller are illustrated in Figure 7 for a step input torque; this applied input is such that the tip rotates through a small angle (of less than  $5^\circ$ , in terms of the rigid position). The values for torque begin at zero, that is, the dc component is subtracted out. In the simulation, the response settles in about ten seconds, whereas the free response decays after about one minute due to damping included in the model.

#### 4. Structure-Mounted Proof-Mass Actuation

Since the large-angle slewing problem is complicated due to the flexibility effects inherent in the structure to be slewed, one is naturally led to investigate the possibility of *relegating*, at least partially, the task of vibration damping to a separate sensor-actuator pair and associated feedback loop. To this end, we have been investigating utilization of a structure-mounted momentum-exchange device mounted near the tip of the single-link manipulator. The practicality of such active vibration damping in a robotic environment is closely coupled to the availability of lightweight and effective devices. The device we have considered in our preliminary studies is a proof-mass actuator developed in our labs to study active vibration in space based flexible mechanical structures.

Non-ground referenced linear actuators are not yet widely available on the market, and this fact led to an in-house development; a general view of the device as mounted on the arm is shown in Figure 8. The device is built around a linear motor manufactured by the Kimco division of BEI Motion Systems which has a total mass of 25 grams, and can deliver a peak force of 2.2 N. The coil (solenoid) is rigidly mounted to a beam clamp which fixes the actuator to the arm. Also connected to the clamp is a rigid aluminum bracket which supports the springs. The proof mass is coupled to the framework through the springs, which are in turn coupled to the framework with adjusting screws so that their rest tension and proof mass rest position can be controlled. There is sufficient adjustment so that springs of different length and stiffness constant can be accommodated. The springs provide a restoring force for the proof mass and transfer force to the structure. A hanger was also mounted to provide strain relief for the feed wires.

The proof mass consists of a rectangular steel ring with a central steel member. This central member passes through the coil and restricts motion to a single axis. Samarium cobalt magnets are fixed to the top and bottom inside edges of the ring (adjacent to the coil) so that the interaction of the permanent magnetic field with a current in the coil results in a force on the proof mass.

Details of the development of the dynamic model of the actuator may be found in [17]. The net force applied to the tip of the arm (where the actuator is mounted) may be given as

$$f = 2kz - K_f \dot{z} + B\ddot{z}, \quad (13)$$

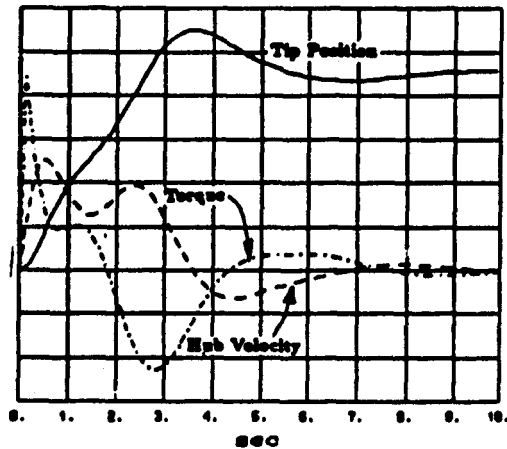


Figure 7: Output Feedback Example

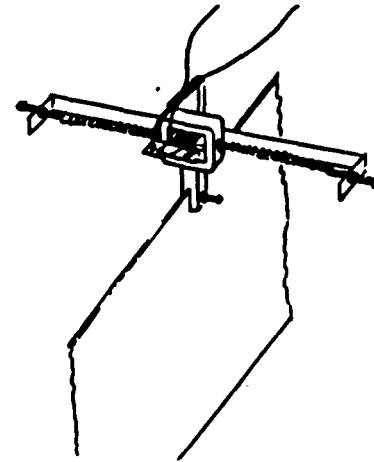


Figure 8: OSU Proof-Mass Actuator

$$m\ddot{z} + B\dot{z} + 2kz = K_F i + m\ddot{y} \quad (14)$$

where  $m$  is the proof mass,  $y$  the displacement of the structure at the point of actuator attachment,  $f$  the force acting at that point,  $z$  the relative displacement of the proof mass,  $B$  the viscous damping coefficient,  $K_F$  the motor force constant, and  $i, i_a$  are the input and armature currents, respectively. The actuator constants taken from the data sheets which accompany the individual components, are  $m = 0.0207$  kg,  $k = 262.7$  N-m<sup>-1</sup>,  $K_F = 1.112$  N-ampere<sup>-1</sup>. The incorporation of the above actuator creates a second feedback loop to which the task of vibration damping is *relegated*. The two control loops (for slewing and for vibration damping) can be both designed and implemented in a decentralized manner. Note that  $y$  includes the displacement due to both the rigid body mode and the flexibility (see (1)). The principle of *relegation* implies that we design the feedback control only for the latter portion. To this end consider a vibration damping loop for only the first mode, such that the relevant expression is

$$\ddot{q}_1 + \omega_1^2 q_1 = b_1 f \quad (15)$$

where  $\omega_1$  is the natural frequency of the first mode and  $b_1$  is an influence factor determined from the mode shape at the point of interest. Acceleration feedback can be used from the co-located accelerometer and a simple PI controller has been designed. It is evident, however, that the STAC approach or the frequency weighted control approach outlined earlier, can also be used here. The incorporation of the more sophisticated design approaches resulting in more complicated controllers will aid in handling more than the first vibrational mode. Studies along this direction are presently continuing.

## 5. Conclusion

In this workshop presentation we have described work in progress on modeling, parameter estimation, and control studies for an experimental, one-meter single-link flexible manipulator arm. Models have been developed for the apparatus based on finite element analysis and experimental verification. These, with the closed-loop parameter estimation procedures described here, and subsequent STAC approach for control, are being evaluated on the laboratory arm.

Under investigation is experimentation involving local proof-mass actuation for vibration control at the tip of the arm, using a device developed in the Control Research Laboratory at Ohio State for flexible structures control work. The output feedback frequency shaping approach described here may be easily extended to this application, where the formulation is *decentralized* in nature; results on this technique for general flexible structure vibration control will appear in [25]. Finally, various other centralized (for the case of hub actuation only) and decentralized approaches are currently being evaluated in the laboratory.

## References

- [1] H. Kanoh and H. Lee, "Vibration control of a one-link flexible arm," in *Proceedings of the 24th Conference on Decision and Control*, pp. 1172-1177, Ft. Lauderdale, Florida, December 1985.
- [2] P. Kärkkäinen, "Compensation of manipulator flexibility effects by modal space techniques," in *Proceedings of the IEEE International Conference on Robotics and Automation*, pp. 972-977, St. Louis, MO, April 1985.
- [3] R. Marino and M. W. Spong, "Nonlinear control techniques for flexible joint manipulators: A single link case study," in *Proceedings of the IEEE International Conference on Robotics and Automation*, pp. 1030-1036, San Francisco, April 1986.

- [4] A. Barraco, B. Curry, and G. Ishiomin, "Dynamic control for flexible robots: Different approaches," in *Proceedings of the IEEE International Conference on Robotics and Automation*, pp. 1038-1043, San Francisco, April 1986.
- [5] R. P. Judd and D. R. Falkenburg, "Dynamics of nonrigid articulated robot linkages," *IEEE Transactions on Automatic Control*, vol. AC-30, no. 5, pp. 499-502, May 1985.
- [6] K. Khorasani and M. W. Spong, "Invariant manifolds and their application to robot manipulators with flexible joints," in *Proceedings of the IEEE International Conference on Robotics and Automation*, pp. 978-983, St. Louis, MO, April 1985.
- [7] A. D. Luca, A. Isidori, and F. Nicolo, "Control of a robot arm with elastic joints via nonlinear dynamic feedback," in *Proceedings of the 24th Conferences on Decision and Control*, pp. 1671-1679, Ft. Lauderdale, December 1985.
- [8] W. J. Book and M. Majette, "Controller design for flexible, distributed parameter mechanical arms via combined state space and frequency domain techniques," *Journal of Dynamic System, Measurement, and Control*, vol. 105, pp. 245-254, December 1983.
- [9] G. G. Hastings and W. J. Book, "Experiments in optimal control of a flexible arm," in *Proceedings of the 1985 American Control Conference*, pp. 728-729, Boston, MA, June 1985.
- [10] G. G. Hastings and W. J. Book, "Verification of a linear dynamic model for flexible robotic manipulators," in *Proceedings of the IEEE International Conference on Robotics and Automation*, pp. 1024-1029, San Francisco, CA, April 1986.
- [11] W. J. Book, S. Cetinkunt, and G. W. Woodruff, "Near optimum control of flexible robot arms on fixed paths," in *Proceedings of the 24th Conference on Decision and Control*, pp. 1522-1528, Ft. Lauderdale, December 1985.
- [12] D. Schaechter, "Hardware demonstration of flexible beam control," *Journal of Guidance and Control*, vol. 5, no. 1, pp. 48-53, January 1982.
- [13] D. Eldred and D. Schaechter, "Experimental demonstration of static shape control," *Journal of Guidance and Control*, vol. 6, no. 3, pp. 188-192, May 1983.
- [14] R. H. Canon and E. Schnütz, "Initial experiments on the end-point control of a flexible one-link robot," *The International Journal of Robotics Research*, vol. 3, no. 3, pp. 62-75, 1984.
- [15] J. Juang, L. G. Horta, and H. H. Robertshaw, "A slewing control experiment for flexible structures," in *Proceedings of the Fifth VPI & SU AIAA Symposium on Dynamics and Control of Large Structures*, Blacksburg, VA, June 1985.
- [16] J. N. Juang, J. D. Turner, and H. M. Chun, "Closed-form solutions for feedback control with terminal constraints," *Journal of Guidance and Control*, vol. 8, no. 1, pp. 39-43, January 1985.
- [17] J. Martin, U. Özgüner, and S. Yurkovich, "An active vibration damper for flexible structures," in *Proceedings of the Seventeenth Annual Pittsburgh Conference on Modeling and Simulation*, April 1986.
- [18] R. W. Gorman, *ANSYS Engineering Analysis System PC/ED. User's Manual*. Swanson Analysis Systems, Inc., 1985.
- [19] R. J. Ulman, "System identification studies for flexible structures," M.S. Thesis, The Ohio State University, 1986.
- [20] U. Özgüner, S. Yurkovich, J. Martin, and F. Al-Abbass, "Decentralized control experiments on NASA's flexible grid," in *Proceedings of the 1986 American Control Conference*, pp. 1045-1051, Seattle WA, June 1986.
- [21] A. Tzes and S. Yurkovich, "A sensitivity analysis approach to the control of manipulators with unknown load," in *Proceedings of the IEEE International Conference on Robotics and Automation*, Raleigh, NC, March 1987. (to appear).
- [22] D. Schaechter, "Optimal local control of flexible structures," *Journal of Guidance and Control*, vol. 4, no. 1, pp. 22-26, January 1981.
- [23] S. Yurkovich, U. Özgüner, and F. Al-Abbass, "Sliding mode, model reference adaptive control for flexible structures," Technical Report CRL-1008-Su86-P, The Ohio State University, Control Research Laboratory, 1986.
- [24] N. K. Gupta, "Frequency-shaped cost functionals: Extension of linear-quadratic-Gaussian design methods," *Journal of Guidance and Control*, vol. 3, no. 6, pp. 529-535, November 1980.
- [25] U. Özgüner and S. Yurkovich, "Decentralized frequency shaping and model sensitivities for optimal control of large space structures," in *Proceedings of the 10th IFAC World Congress*, Munich, West Germany, July 1987. (to appear).